Investigations of diatrizoate degradation by photo-activated persulfate

Lei Zhou, Mohamad Sleiman, Corinne Ferronato, Jean-Marc Chovelon, Claire Richard

Investigations of diatrizoate degradation by photo-activated persulfate Lei

Zhou [a], Corinne Ferronato [a], Jean-Marc Chovelon [a,*], Mohamad Sleiman [b,c], Claire Richard [c,d,*]

[a] Univ Lyon, Université Claude Bernard Lyon 1, CNRS, IRCELYON, F-69626 Villeurbanne, France
[b] Université Clermont Auvergne, Sigma-Clermont, Institut de Chimie de Clermont-Ferrand, BP 10448, F-63000 Clermont-Ferrand, France
[c] CNRS, UMR 6296, ICCF, F-63178 Aubière, France
[d] Université Clermont Auvergne, Université Blaise Pascal, Institut de Chimie de Clermont-Ferrand, BP 10448, F-63000 Clermont-Ferrand, France

The widespread occurrence of iodinated X-ray contrast media (ICMs) in aquatic systems poses potential risks to ecologic system and human health. The present study investigated the degradation kinetics and mechanisms of a typical ICMs, diatrizoate (DTZ), by using simulated sunlight (from a solar simulator Suntest CPS+) activated persulfate (PS) oxidation process. The influence of key kinetic factors, such as PS concentrations, pH, dissolved organic matter (DOM), bicarbonate and chloride ions was evaluated. The reaction pathways and mechanisms were proposed based on photoproducts identification using HPLC-MS. UV/PS was found to be more efficient than UV/H_2O_2. Sulfate radicals ($SO_4^{\cdot-}$) was the dominant reactive species in the oxidation process, and the second-order rate constant of sulfate radical with DTZ was calculated as1.90×10^9 M^{-1} s^{-1} based on laser flash photolysis (LFP) experiments. The results indicated that increasing initial PS concentration favored the decomposition of DTZ; whereas, degradation of DTZ was not affected by pH change ranging from 4.5 to 8.5. DOM inhibited DTZ removal rate, while, bicarbonate enhanced it, and chloride ions induced a negative effect above 500 mM. Major oxidation pathways including deiodination-hydroxylation, decarboxylation- hydroxylation and side chain cleavage were proposed, and detailed underlying mechanisms were also discussed. We suggest a direct photodegradation of primary intermediates generated by $SO_4^{\cdot-}$ attack. These findings demonstrate that halogenated pollutants can readily react with $SO_4^{\cdot-}$ to form light-absorbing intermediates (ranging from 350 to 500 nm). Thus, this activation method could be a promising approach in the removal of ICMs.

1. Introduction

In recent decades, a growing number of studies have documented the widespread occurrence of pharmaceuticals in aquatic environment, raising serious concerns about their influence on aquatic ecosystems and human health [1–4]. Many pharmaceuticals were found to be recalcitrant to conventional drinking water and wastewater treatment processes (WWTPs) [5,6]. As a consequence, pharmaceuticals are frequently detected in natural waters, and in drinking waters and constitute a potential risk for human health [7–11].

Iodinated X-ray contrast media (ICMs), a class of medical diagnostic agents routinely prescribed for imaging tissues and internal, are among the most recalcitrant and highly persistent pharmaceuticals [5]. Large quantities of ICM are administered to individual patients undergoing tests (>100 g $dose^{-1}$), and the annual worldwide consumption of ICMs was reported as approximately 3.5×10^6 kg [12]. ICMs are designed to be resistant to metabolism and thus are generally excreted unchanged within 24 h [13].

* Corresponding authors.
E-mail addresses: lei.zhou@ircelyon.univ-lyon1.fr (L. Zhou), jean-marc.chovelon@ircelyon.univ-lyon1.fr (J.-M. Chovelon), claire.richard@univ-bpclermont.fr (C. Richard).

Conventional WWTPs could not remove ICMs effectively, leading to their occurrence in surface water and ground water at concentration ranging from ng L^{-1} to μg L^{-1} [14–17]. The ICMs contribute substantially to the organic halogen levels in municipal and hospital effluents, which has raised additional concerns [18]. The published information about the environmental risk of ICMs is not abundant, however, some research has shown that DTZ may have nephrotoxic effects in animals and humans [19,20]. Although there is lack of information about their impact on health, drinking water should be free of ICMs to minimize the potential risk of long-term adverse health effects. Therefore, it is essential to develop an effective treatment technology to remove these compounds from waters.

Advanced oxidation processes (AOPs) are promising alternatives capable of removing these pharmaceuticals from WWTPs. The AOPs technology is mainly based on the generation of reactive species arising from the decomposition of oxidants such as hydrogen peroxide (H_2O_2) and persulfate (PS, $S_2O_8^{2-}$). Among the commonly used oxidants, PS received wide attention due to its high redox potential ($E^0 \sim 2.1$ V) [21,22]. PS is a relatively stable oxidant in water, however, it can be activated by UV, heat, base, or transition metals to generate a stronger oxidant, sulfate radical ($SO_4^{\cdot-}$, $E^0 \sim 2.6$ V) [23–27]. It has been demonstrated that, $SO_4^{\cdot-}$, in general, could react with organic compounds with a second-order rate constant in the range 10^6–10^9 M^{-1} s^{-1} [28]. Unlike the well-known hydroxyl radical (·OH), $SO_4^{\cdot-}$ is believed to react with organic compounds mainly via electron transfer mechanism, which makes it more selective [29]. Moreover, by comparison with ·OH, $SO_4^{\cdot-}$ is less likely scavenged by dissolved organic matter (DOM), such as humic and fulvic acids, that are ubiquitously present in natural waters [30]. Therefore, $SO_4^{\cdot-}$ -based oxidation processes show advantageous relative to conventional HO·-based AOPs in certain water treatment and remediation scenarios [31].

Various AOPs processes have been utilized to degrade ICMs, such as UV/H_2O_2, UV/TiO_2, O_3 [32–34]. While treatment feasibility of ICMs was examined, previous studies did not provide mechanistic details and did not explore the effects of naturally occurring substances (e.g., DOM, bicarbonate), which are essential for optimizing the treatment process. Moreover, studies reporting the treatment of ICMs by $SO_4^{\cdot-}$-based oxidation process, especially ionic ICM like diatrizoate (DTZ) that was remarkably resistant to biodegradation, are scarce [35,36]. Velo-Gala *et.al* undertook a comparative study on different AOPs processes for the degradation of DTZ, and found that $SO_4^{\cdot-}$-based oxidation process could be an effective choice [37]. However, a detailed kinetic and mechanistic map describing the degradation of DTZ by $SO_4^{\cdot-}$ is still lacking.

In the present study, we attempted to elucidate the underlying mechanisms and oxidation pathways of the reaction between DTZ and $SO_4^{\cdot-}$. $SO_4^{\cdot-}$ was generated by simulated sunlight activated PS process. Kinetic studies were conducted for a better understanding of the influence of factors including pH and natural water constituents. The identification of DTZ transformation intermediates and products was also performed by using HPLC-MS method. Based on the HPLC-MS data, the reaction mechanisms and detailed transformation pathways were proposed. Our study provides useful information about using sulfate radical-based technologies for remediation of the groundwater contaminated by DTZ and structurally related X-ray contrast agent.

2. Materials and methods

2.1. Chemicals

Sodium diatrizoate hydrate (DTZ, 98%), nitrobenzene (NB, 99%), *para*-nitroaniline (PNA, 99%), hydrogen peroxide (30% w/w) and potassium persulfate ($K_2S_2O_8$, 99%) were purchased from Sigma-Aldrich. Suwannee River fulvic acid (SRFA, 1R101F) of reference grade was obtained from International Humic Substance Society (IHSS). HPLC or LC–MS grade acetonitrile (ACN), methanol (MeOH), ethanol (EtOH) and *t*-butanol (TBA) were supplied by Fisher Chemical. Other reagents were of analytical grade and used as received without further purification. Milli-Q water (18 MΩ cm) was prepared from a Millipore Milli-Q system. All solutions were prepared by dissolving the chemical agents into Milli-Q water without further purification.

2.2. Experiments setup

$SO_4^{\cdot-}$ radicals were generated by activation of persulfate under simulated solar irradiation, and the irradiation experiments were conducted in a solar simulator Suntest CPS+, (HERAEUS, Hanau, France) equipped with a 1.5 kW xenon arc and an ultraviolet filter allowing a simulation of the solar spectrum between 290 nm and 400 nm. The reaction was carried out in a cylindrical Pyrex reactor (i.d. = 5 cm, H = 15 cm, V = 150 mL) and the temperature was maintained at 20 °C using a circulating water system. A scheme of the applied reactor is present in Fig. S1 (Supplementary Material). Specific aliquot of substrate (DTZ) and appropriate volumes of persulfate stock solution were added to achieve 50 mL reaction solution. Control experiments with substrates alone and dark experiments with substrate-persulfate were carried out under identical conditions. Except for buffered solutions (achieved using 10 mM Na_2HPO_4 and 10 mM NaH_2PO_4 in the experiments with bicarbonate), the initial pH of other reaction solutions were adjusted using 0.01 M H_2SO_4 and 0.01 M NaOH. Aliquots of 0.3 mL were withdrawn at selected time intervals and quenched immediately with the same volume of methanol, a well-known scavenger for $SO_4^{\cdot-}$ and ·OH, to stop the chemical oxidation reactions. All experiments were performed at least in duplicate.

2.3. Analytical procedures

The concentrations of DTZ, NB and PNA were analyzed using a Shimadzu 10A series high performance liquid chromatography (HPLC, Shimadzu) system equipped with a Model 7725i injector with a 20 μL sample loop and coupled with a LC-10AT binary pump and a SPD-M10ADAD. Samples were separated using an Ypersphere BDS C_{18} column (5 μm, 125 mm * 4.0 mm, i.d.) (Interchim, France) at 40 °C. The mobile phase was a mixture of acetonitrile and acidified-water (3‰ formic acid by volume, pH 3.0). An overview of the HPLC parameters is given together in Table S1, Supplementary Material.

Concentrations of SRFA were expressed as total organic carbon (TOC, mg C L^{-1}) and determined using a Shimadzu 5000A analyzer (Japan).

The UV–vis spectra of the selected chemicals were recorded using a Lambda 950 UV–vis spectrophotometer (PerkinElmer, USA) and quartz cuvettes.

Identification of the degradation products of DTZ were carried out using HPLC-MS method. The HPLC-MS data were recorded using an Agilent Chromatograph equipped with a 996-photodiode array detector, an atmospheric-pressure chemical ionization device (APCI), and a reverse Zorbax eclipse $XDDC_{18}$ column (5 μm, 150 mm * 4.6 mm, i.d.).

The pH of the solutions was measured using a combined glass electrode connected to a PHM 210 Standard pH meter (Radiometer, Copenhagen).

The second order rate constant of DTZ with $SO_4^{\cdot-}$ was determined by means of laser flash photolysis (LFP) by recording the $SO^{\cdot-}$ decay rates under different conditions. The rate constants of

DTZ with ·OH and CO_3^{-} were calculated by competitive kinetic methods. The detailed description of these methods are presented in Supplementary Material (Text S1–S3).

PS concentration was evaluated by a spectrophotometric method, which is presented in Text S6, Supplementary Material. PS in excess was used in our study and the change of PS concentration within 60 min was negligible. Concentration of sulfate radical at the initial step was also calculated by the method described in Text S8, Supplementary Material, and the values are listed in Table S4.

3. Results and discussion

Preliminary dark control experiments with DTZ and PS were conducted (in Fig. 1). No loss of DTZ was observed, indicating that no reaction occurs in the absence of light activation.

3.1. Reaction kinetics

Before investigating the AOPs process, we studied the photolysis of DTZ alone in the solar simulator. As shown in Fig. 1, the decay of DTZ was negligible, in accordance with the work by Sugihara et al. who showed that DTZ did not undergo photolysis under UVA irradiation [38]. From this point on, the discussion will focus on the indirect photolysis for a more straightforward comparison on reactive species' contributions under different conditions.

3.1.1. Comparison of UV/H_2O_2 and UV/PS oxidation

Fig. 1 exhibits the degradation of DTZ treated by UV/H_2O_2 and UV/PS, respectively. In both cases, the degradation of DTZ was significant in the first 20 min, afterwards the rate of DTZ disappearance slowed down. Such an auto-inhibition of the reaction has been reported for many compounds during oxidation processes by sulfate radical, such as diuron [23], polychlorinated biphenyls [42], atrazine [50], methylene blue [61] and tetrabromobisphenol A [62].

The presence of H_2O_2 led to the removal of 17% of DTZ after 1 h of irradiation. The degradation could be attributed to the generation of highly oxidizing radical species, ·OH. Indeed, when excess methanol (100 mM, as ·OH scavenger) was added in the solution, the oxidation of DTZ was inhibited by more than 95%.

On the other hand, 42% of DTZ was degraded when using UV/PS after 1 h of irradiation. The degradation of DTZ was mostly due to the formation of sulfate radical (SO_4^{-}) (Eqs. (1) and (2)), where P represents the oxidation products.

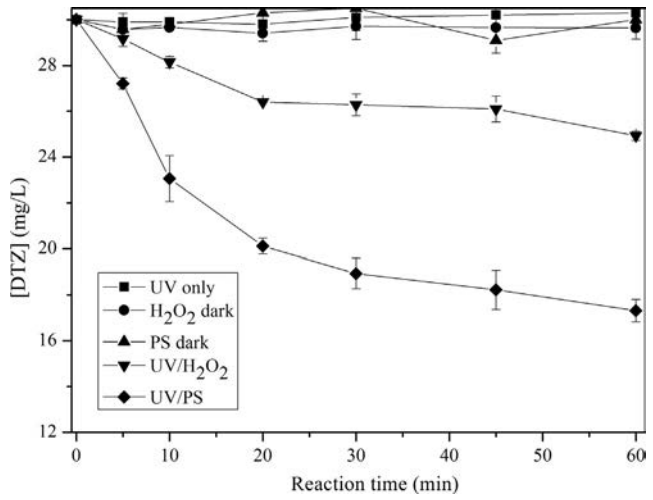

Fig. 1. Degradation of DTZ by UV, H_2O_2 in dark, PS in dark, UV/H_2O_2 and UV/PS. ([DTZ]$_0$ = 30 mg L^{-1}, [H_2O_2]$_0$ = [PS]$_0$ = 12 mM, initial pH = 6.5).

$$S_2O_8^{2-} + h\nu \rightarrow 2SO_4^{-} \quad (1)$$

$$DTZ + SO_4^{-} \rightarrow P,\ k_0 = 1.90 \times 10^9\ M^{-1}\ s^{-1} \quad (2)$$

The second order rate constant for DTZ with SO_4^{-} was determined as $(1.9 \pm 0.2) \times 10^9\ M^{-1}\ s^{-1}$ by means of laser flash photolysis (see Supplementary Material). For the reaction with ·OH, the value of $(6.1 \pm 0.1) \times 10^8\ M^{-1}\ s^{-1}$ was calculated (also in Supplementary Material), which was in accordance with literature data (ranging from 5.40 to $9.58 \times 10^8\ M^{-1}\ s^{-1}$) [33,39]. The rate constant is slower than that with SO_4^{-}, demonstrating that using activated persulfate to generate SO_4^{-} could be a much more effective way to remove DTZ. PS was much effective than H_2O_2 for the removal of DTZ under solar irradiation under neutral conditions. Similar results were also found in a previous study, the degradation rate of DTZ by UV/PS is 30% faster than that by UV/H_2O_2 [37]. The higher performance of PS can be attributed to its higher light absorption in the wavelength range of simulated solar light emission spectra. For instance, the molar extinction coefficient of PS, ε, is equal to 0.68 $M^{-1}\ cm^{-1}$ at 310 nm, against 0.42 $M^{-1}\ cm^{-1}$ for H_2O_2.

In our study, the deceleration of DTZ degradation can be attributed to the formation of oxidation products, which could affect the reaction through two different ways. Firstly, the light-absorbing products would compete with PS for light flux, thereby reducing the yield of SO_4^{-}. Secondly, oxidation products could also compete with DTZ for the reaction with SO_4^{-}. These competitive reactions should slow down the decomposition rate of DTZ.

$$P_i + SO_4^{-} \rightarrow P_j,\ k_i \quad (3)$$

In the first stages of the reaction, if we assume that sulfate radicals only react with DTZ, the rate of DTZ degradation could be written:

$$-\frac{d[DTZ]}{dt} = I_{PS}^0 \Phi \quad (4)$$

where I_{PS} is the light intensity absorbed by PS and Φ, is the quantum yield of sulfate radical formation. In the course of the reaction, when oxidation products compete with DTZ for sulfate radical, the rate law becomes:

$$-\frac{d[DTZ]}{dt} = I_{PS}\Phi \frac{k_0[DTZ]}{\sum_{1}^{i} k_i[P_i] + k_0[DTZ]} \quad (5)$$

where P_i are the oxidation products and k_i are their reaction rate constants with SO_4^{-}.

The decay of I_{PS} has been calculated based on the UV–Vis spectra of the reaction solution (detailed description in Text S7 and result in Fig. S10, Supplementary Material). The result indicated that after 1 h of irradiation, I_{PS} was reduced by 20–25%. From Fig. 4 we could know that several phenolic products were generated in the reaction. As electron-rich compounds, phenolic compounds could react with sulfate radical at rates higher than that of the mother compound, DTZ [59]. Considering Eqs. (4) and (5), the rate of DTZ degradation should decrease when products accumulate in the medium.

3.1.2. Effects of initial solution pH and initial PS concentrations

In real-world applications, pH conditions are expected to be variable, a fixed pH is not realistic. Therefore, we assessed the kinetic of DTZ degradation under different initial pH values (4.5–10.5).Summarized results are presented in Table S2, Supplementary Material. Overall, the increase of pH from 4.5 to 8.5 did not

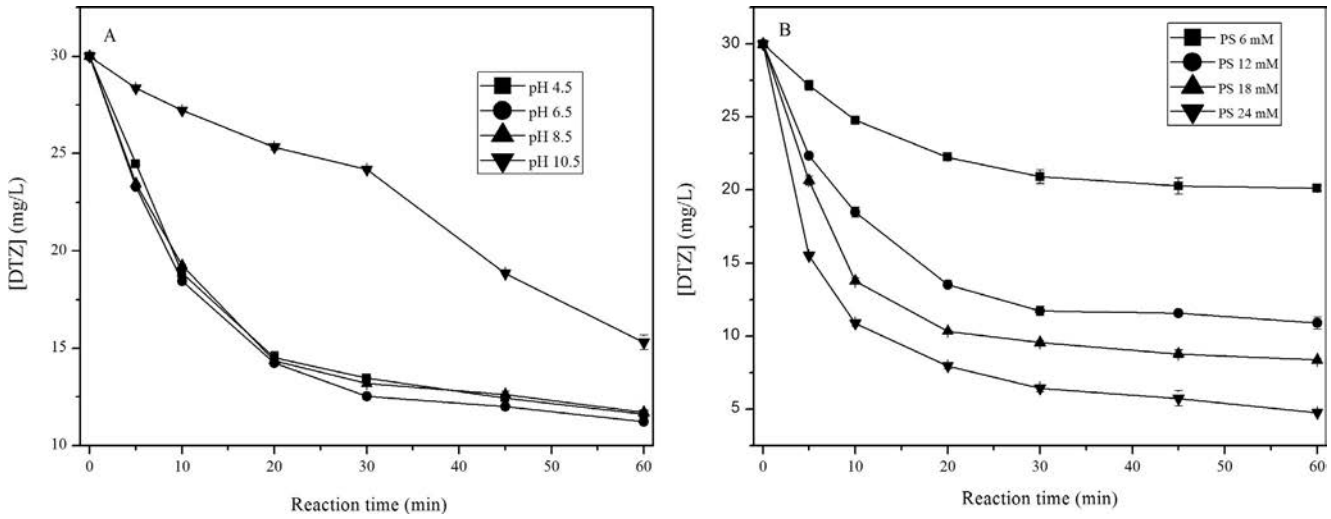

Fig. 2. Degradation of DTZ by UV/PS (A) for various pH, ($[DTZ]_0$ = 30 mg L^{-1}, $[PS]_0$ = 12 mM); (B) for different initial PS doses ($[DTZ]_0$ = 30 mg L^{-1}, initial pH = 6.5).

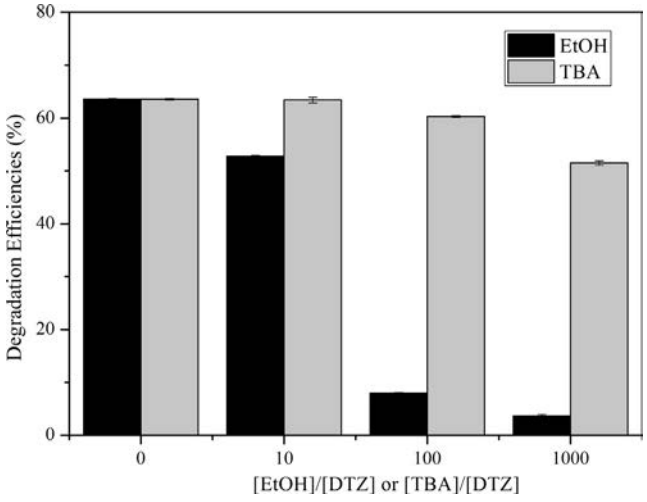

Fig. 3. Degradation efficiencies of DTZ by UV/PS in the presence of different scavengers (EtOH and TBA) molar ratios. ($[DTZ]_0$ = 30 mg L^{-1}, $[PS]_0$ = 12 mM, initial pH = 6.5, reaction time = 60 min).

affect the removal efficiency of DTZ, which remained in the range 61–63%. However, the oxidation was found to decline at pH 10.5, as only 49% of DTZ was removed. This result is consistent with previous report where high pH values (pH 12) slowed the degradation of DTZ by UV/PS compared with neutral and acidic conditions [37]. In addition, it is worthy to note that the solution pH in all experiments decreased during the reaction process, mostly due to the decomposition of PS and the formation of acidic species.

Solution pH might play a complex role in sulfate radical based oxidation process on organic contaminants since it could affect the ionization state of organic compounds as well as the formation of reactive species (i.e. $SO_4^{\cdot-}$ and ·OH) [40]. Depending on the pH, DTZ can exist in up to six different acid-base forms (Fig. S2, Supplementary Material). When the solution pH is higher than 6, the form in which three H^+ are removed (No 6 in Fig. S2) is the dominant species with a contribution larger than 90%. Although all the samples (pH ranging from 4.5 to 10.5) underwent acidification during the reaction, for the last 3 groups (pH 6.5, 8.5 and 10.5), the reaction solutions experienced a similar change of DTZ species during the reaction. We could conclude that the speciation of DTZ was not responsible for the inhibition of oxidation at pH 10.5.

Since the decline of DTZ removal rate could not be attributed to the effect of pH on oxidation efficiency, the evolution of reactive species during the reaction was taken into consideration. It has been demonstrated that $SO_4^{\cdot-}$ can yield ·OH under neutral or basic conditions (Eqs. (6) and (7)) [41,42].

$$SO_4^{\cdot-} + H_2O \rightarrow SO_4^{2-} + {}^{\cdot}OH + H^+ \; k[H2O] < 2 \times 10^3 \; s^{-1} \quad (6)$$

$$SO_4^{\cdot-} + OH^- \rightarrow SO_4^{2-} + {}^{\cdot}OH \; k \approx 6.5 \times 10^7 \; M^{-1} \; s^{-1} \quad (7)$$

The formation of ·OH in basic conditions could partly explain the decline of DTZ degradation, since the second order rate constant of DTZ with ·OH was smaller ($6.1 \times 10^8 \; M^{-1} \; s^{-1}$) than that with $SO_4^{\cdot-}$ ($1.9 \times 10^9 \; M^{-1} \; s^{-1}$) [33,39,43]. Another possible explanation of the pH effect is the base-activated PS decomposition described by Eq. (8) [24].

$$2S_2O_8^{2-} + 4OH^- \rightarrow SO_4^{\cdot-} + 3SO_4^{2-} + O_2^{\cdot-} + 2H_2O \quad (8)$$

The yield of $SO_4^{\cdot-}$ *via* base-activated persulfate is much lower than that from UV-activated persulfate (Eq. (3)) as only one $SO_4^{\cdot-}$ radical is generated per 2 PS molecules. The competition of these two reactions inevitably decreased the concentration of $SO_4^{\cdot-}$, as well as that of ·OH. Zhang et al. confirmed this reduction by determining the steady-state concentrations of $SO_4^{\cdot-}$ and ·OH ($[SO_4^{\cdot-}]_{ss}$ and $[{}^{\cdot}OH]_{ss}$) by UV/PS under different pH values [44]. They found that both $[SO_4^{\cdot-}]_{ss}$ and $[{}^{\cdot}OH]_{ss}$ values were lower in basic than neutral conditions. At pH 8.5, due to the relatively low concentration of OH^- ($\approx 4.2 \times 10^{-6}$ M at beginning, and would continue to decrease during the reaction), the effect of these two reactions was indistinctive, which made the removal efficiency of DTZ among the range of pH 4.5–8.5 was nearly identical.

3.1.3. Effects of solution PS dose

Table S2 lists the degradation efficiencies of 30 mg L^{-1} DTZ by UV activated PS for different PS concentrations. Increasing the initial PS concentration significantly enhanced the degradation efficiency of DTZ. This result suggests that higher PS concentration yielded higher level of $SO_4^{\cdot-}$ by UV activation, promoting the oxidation of DTZ.

Some previous studies have reported that an increase of the initial PS concentration could not continuously ensure an increase of the decomposition efficiency due to the scavenging of $SO_4^{\cdot-}$ by $S_2O_8^{2-}$ (Eq. (9)), especially under acidic conditions [45–47].

$$S_2O_8^{2-} + SO_4^{\cdot-} \rightarrow SO_4^{2-} + S_2O_8^{\cdot-}, \; k_5 = 5.5. \times 10^5 \; M^{-1} \; s^{-1} \quad (9)$$

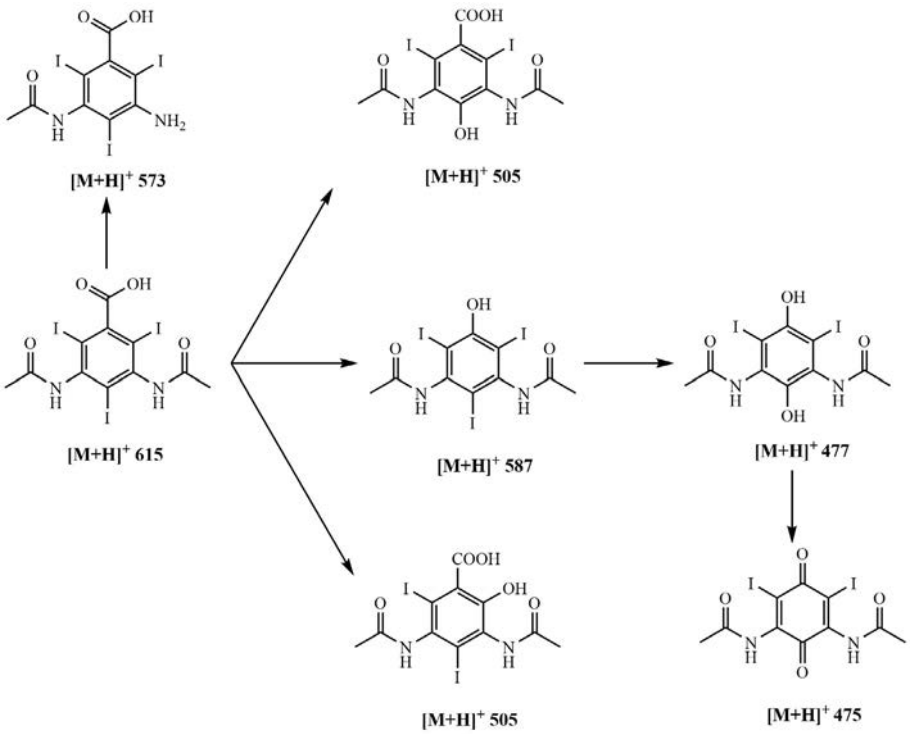

Fig. 4. Proposed oxidation pathways of DTZ by simulated sunlight activated PS. ($[DTZ]_0$ = 30 mg L^{-1}, $[PS]_0$ = 12 mM, pH = 6.5, reaction time = 60 min).

However, this inhibiting effect of PS was not observed in the present work. Laser flash photolysis experiments were conducted (in the absence of DTZ) to better elucidate the scavenging effect of persulfate anions. The decay rates of $SO_4^{\cdot-}$ decay were found to be 1.7, 2.0, 1.7, 1.8, 1.7 and 1.8 × 10^5 s^{-1} at PS concentration of 6, 12, 24, 30, 36 and 44 mM, respectively. If the scavenging effect of PS played a role in the reaction process, the decay rate should increase with the increasing of PS concentrations. The highest PS initial concentration used in our work did not reach the critical level to slow down the degradation rate constant of DTZ.

3.2. Identification of oxidizing species ($SO_4^{\cdot-}$ and ·OH)

The DTZ loss mentioned above suggests that reactive species were produced by PS under simulated sunlight irradiation. $SO_4^{\cdot-}$ and ·OH can be considered as the main oxidizing species involved in the decomposition process of DTZ.

A better understanding of the contribution of each of these radicals in the reaction was evaluated by using specific scavengers like ethanol (EtOH) and tert-butyl alcohol (TBA) [48,49]. The bimolecular rate constants of reaction of these two scavengers with the radicals are given in Eqs. (10)–(13). EtOH is a more efficient quencher than TBA, and both alcohols quench ·OH more easily than $SO_4^{\cdot-}$.

$$\mathrm{EtOH} + SO_4^{\cdot-} \rightarrow \text{intermediates},\ k_{10} = (1.6 - 7.7) \times 10^7\ \mathrm{M^{-1}s^{-1}} \quad (10)$$

$$\mathrm{EtOH} + {}^{\cdot}\mathrm{OH} \rightarrow \text{intermediates},\ k_{11} = (1.2 - 2.8) \times 10^9\ \mathrm{M^{-1}\ s^{-1}} \quad (11)$$

$$\mathrm{TBA} + SO_4^{\cdot-} \rightarrow \text{intermediates},\ k_{12} = (4 - 9.1) \times 10^5\ \mathrm{M^{-1}\ s^{-1}} \quad (12)$$

$$\mathrm{TBA} + {}^{\cdot}\mathrm{OH} \rightarrow \text{intermediates},\ k_{13} = (3.8 - 7.6) \times 10^8\ M^{-1}\ \mathrm{s^{-1}} \quad (13)$$

Their inhibiting effect was measured for various [EtOH]/[DTZ] and [TBA]/[DTZ] ratios.

Fig. 3 displays the results. Comparing the degradation efficiencies in the absence and in the presence of the scavengers allows us to determine the contribution of $SO_4^{\cdot-}$ and ·OH in the reaction. Postulating the quasi-stationary state for $SO_4^{\cdot-}$ and ·OH gives Eqs. (14) and (15) in the case where TBA was added.

$$r_{OH} = k_{OH,DTZ}[\cdot\mathrm{OH}][\mathrm{DTZ}] + k_{14}[\cdot\mathrm{OH}][\mathrm{TBA}] \quad (14)$$

$$r_{SO_4^{\cdot-}} = k_{SO_4^{\cdot-},DTZ}[SO_4^{\cdot-}][\mathrm{DTZ}] + k_{13}[SO_4^{\cdot-}][\mathrm{TBA}] \quad (15)$$

This allows the determination of $[SO_4^{\cdot-}]$ and [·OH] and the degradation rate of DTZ can be written as:

$$\begin{aligned} r_{(DTZ)TBA} &= k_{OH,DTZ}[{}^{\cdot}\mathrm{OH}][\mathrm{DTZ}] + k_{SO_4^{\cdot-},DTZ}[SO_4^{\cdot-}][\mathrm{DTZ}] \\ &= \frac{k_{OH,DTZ}[\mathrm{DTZ}]}{k_{OH,DTZ}[\mathrm{DTZ}] + k_{OH,TBA}[\mathrm{TBA}]} r_{\cdot OH} \\ &\quad + \frac{k_{SO_4^{\cdot-},DTZ}[\mathrm{DTZ}]}{k_{SO_4^{\cdot-},DTZ}[\mathrm{DTZ}] + k_{SO_4^{\cdot-},TBA}[\mathrm{TBA}]} r_{SO_4^{\cdot-}} \end{aligned} \quad (16)$$

Here, we used the mean values of k_{12} and k_{13} from Eqs. (12) and (13) to calculate the contribution of $SO_4^{\cdot-}$ and ·OH. For instance, when [TBA]/[DTZ] = 100, $r_{(DTZ)TBA}$ is equal to:

$$r_{(DTZ)TBA} = 0.01 r_{OH} + 0.97 r_{SO_4^{\cdot-}} \quad (17)$$

At this condition ([TBA]/[DTZ] = 100), the contribution of ·OH was negligible. By comparison the degradation efficiency in the absence of TBA with that in the presence of TBA ([TBA]/[DTZ] = 100), we could calculate that $SO_4^{\cdot-}$ plays a dominant role in the oxidation process.

3.3. Degradation products and reaction pathways

Reaction products generated during UV-activated PS oxidation of DTZ were identified by HPLC-MS. The identification was based

on the analysis of the total ion chromatograms (TIC) and the corresponding mass spectra obtained by the positive ion electrospray HPLC-MS. Data are provided in Table S3, and the proposed degradation pathways is illustrated in Fig. 4. As seen, three pathways take place: pathway a) is the side chain cleavage with formation of an NH_2 group, pathway b) is the deiodination-hydroxylation, and pathway c) is the decarboxylation-hydroxylation .

As a strong oxidant, $SO_4^{\cdot-}$ tends to attack electron rich sites of the compound. For the reaction with DTZ, the initial step is expected to be an electron-transfer from DTZ to $SO_4^{\cdot-}$, leading to the generation of SO_4^{2-} and the DTZ radical cation. The hydrolysis of the radical cation produces the corresponding HO-adducts. The ipso addition of –OH at the iodo site would result in the loss of iodine atom, producing the phenolic products with $m/z = 505$ in ES^+ corresponding to $[M+H]^+$ (Fig. 5A). Two peaks at $m/z = 505$ were identified in the TIC spectra, showing that the substitution of I by OH can take place at two different iodo positions. On the other hand, the ipso addition of –OH at the carbon site bearing the carboxylic acid function could generate decarboxylation-hydroxylation, as confirmed by the detection of the peak at $m/z = 587$ in ES^+ (Fig. 5B). These products were also formed by the attack of ·OH on DTZ, which has been reported in previous work of Jeong et al. [39]. Afterwards, the further decarboxylation-hydroxylation of the phenol or the deiodination-hydroxylation process of the decarboxylated photoproduct can occur, producing the hydroquinonic product ($m/z = 477$ in ES^+) and the corresponding quinonic product ($m/z = 475$ in ES^+) through further oxidation.

Moreover, the product $m/z = 573$ in ES^+ was also characterized, corresponding to the loss of 42 mass units from the parent chemical, which was labeled as the aniline product after the cleavage of the side chain.

The UV–vis spectrum change of DTZ solution in the course of the oxidation was also recorded (Figs. S3 and S4). As can be seen, DTZ does not absorb radiations >350 nm. Yet, the absorbance increased during the reaction between 300 and 500 nm, indicating the formation of highly conjugated molecules. The absorbance reached a maximum after around 60 min of reaction, afterwards, it begun to decrease. Even though PS is still present in the solution, the evolution of the reactional mixture could be at least in part attributed to the absorption of the photoproducts absorbing above 350 nm. This absorption can potentially induce the phototransformation of long-wavelength absorbing photoproducts that visibly disappear in Fig. 2, but might also induce or sensitized the degradation of other photoproducts. Thus, the reaction of DTZ with sulfate radical might be the initial step of the total reaction, and the generation of solar light-absorbing compounds being the driven force for an extended photochemical degradation For instance, the transformation of hydroquinone product ($m/z = 477$) to the quinone product ($m/z = 475$) seems more like a photodegradation pathway than a oxidation process by sulfate radical.

3.4. Impacts of natural water constituents

DOM, chloride (Cl^-) and bicarbonate (HCO_3^-) are ubiquitous natural water constituents. The high redox potentials of $SO_4^{\cdot-}$ ($E^0 \sim 2.6$ eV) and ·OH ($E^0 \sim 2.7$ eV) make them very reactive to destroy organic contaminants as well as the various constituents in natural waters, the competing side reactions with water constituents other than the target contaminants could also lead to the consumption of these two radicals, resulting in an unpredictable consequence on the oxidation efficiency. Investigating the impacts of these natural water constituents on target compound will help to understand its degradation in natural waters by AOPs.

3.4.1. Effect of DOM

The simulated sunlight activated PS induced DTZ degradation was investigated in the presence of SRFA, a reference DOM used in aquatic photochemistry, results are illustrated in Fig. 6.

As seen, the degradation of DTZ was almost drastically inhibited by the addition of SRFA, and the oxidation efficiency was still reduced by an increase in SRFA concentration, indicating a concentration-dependent detrimental effect of SRFA on DTZ degradation. The inhibiting effect of DOM on sulfate radical-based oxidation had also been reported in previous studies [30,50]. DOM is known to be a sink of ·OH and $SO_4^{\cdot-}$ due to some functional groups, which were prone to react with these two radicals [50–52]. Thus, the inhibiting effect could be explained by the competitive scavenging of these two radicals by DOM. Another possibility is the light screening effect of DOM, which could strongly weaken the radiant flux necessary for persulfate degradation.

In addition, the second-order reaction rate constant of SRFA with ·OH was reported as 2.7×10^4 L mg C^{-1} s^{-1} [53], which is comparable to those observed for DOM in natural water samples (the average value was 2.5×10^4 L mg C^{-1} s^{-1}[54]). On the other hand, the second-order reaction rate constant of SRFA with $SO_4^{\cdot-}$ was reported as 6.8×10^3 L mg C^{-1} s^{-1} [30]. The lower reactivity of SRFA towards $SO_4^{\cdot-}$ compared with ·OH was explained by the slow H-abstraction reactions by $SO_4^{\cdot-}$ [30]. Consequently, in the presence of DOM, DTZ could be degraded more efficiently by $SO_4^{\cdot-}$ than by ·OH.

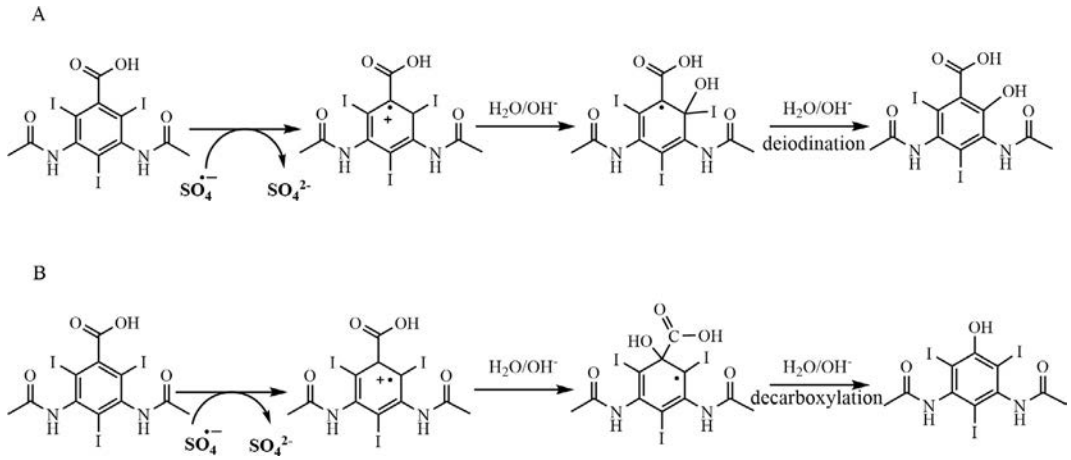

Fig. 5. Proposed oxidation mechanisms of deiodination (A) and decarboxylation (B).

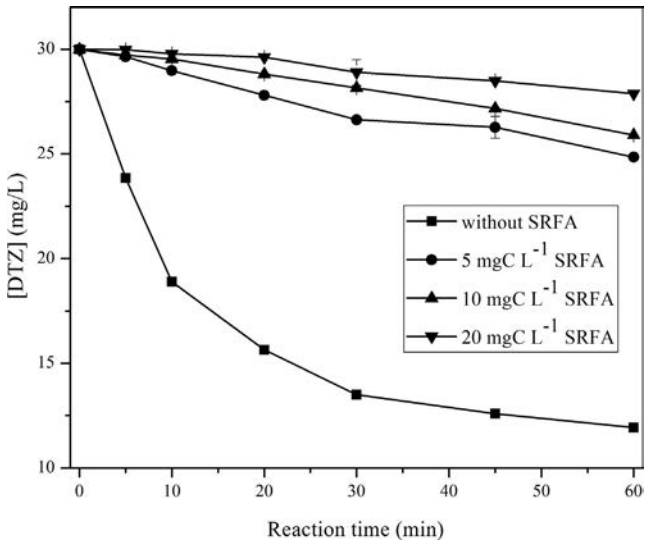

Fig. 6. Decomposition of DTZ by simulated sunlight activated PS in the presence of SRFA. ($[DTZ]_0$ = 30 mg L^{-1}, $[PS]_0$ = 12 mM, initial pH = 6.5, reaction time = 60 min).

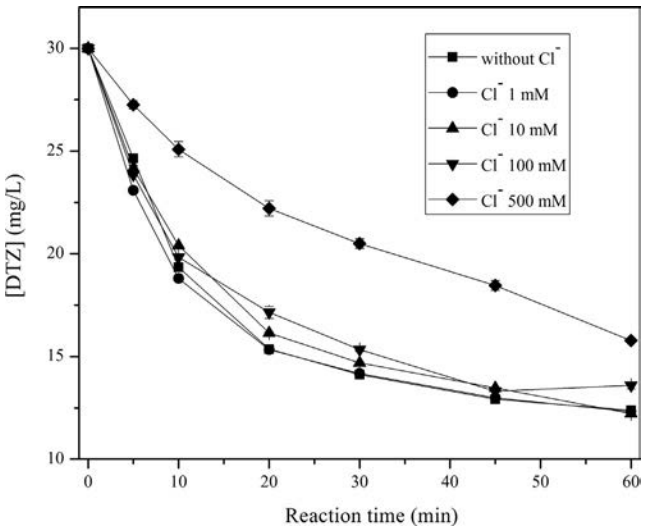

Fig. 7. Decomposition of DTZ by simulated sunlight activated PS in the presence of chloride. ($[DTZ]_0$ = 30 mg L^{-1}, $[PS]_0$ = 12 mM, initial pH = 6.5, reaction time = 60 min).

DOM has been reported to be able to quench the cation radicals of some organic contaminants, such as amino acids, anilines and sulfonamide compounds [55,56]. In the same way, with an aniline structure, cation radical $DTZ^{\cdot+}$, could be reduced by DOM according Eqs. (18) and (19).

$$DTZ + SO_4^{\cdot-} \rightarrow DTZ^{\cdot+} + SO_4^{2-} \quad (18)$$

$$DTZ^{\cdot+} + DOM \rightarrow DTZ + DOM^{\cdot+} \quad (19)$$

Thus, DOM could inhibit the oxidation of DTZ by UV/PS via 3 different mechanisms, including scavenging sulfate radical, light screening effect, and reduction of the intermediates. Among them the light screening effect was dominant, which made the decrease of removal efficiency of DTZ not proportional to the concentrations of SRFA.

3.4.2. Effect of chloride

Chloride ion might play a complex role in $SO_4^{\cdot-}$ based oxidation process due to the scavenging of $SO_4^{\cdot-}$ and ·OH to generate less reactive chlorine species such as Cl·, $ClOH^{\cdot-}$, and $Cl_2^{\cdot-}$ [29,57,58]. As shown in Fig. 7, the effect of chloride ions on the degradation of DTZ at chloride concentrations ranging from 0 to 100 mM was very poor. However, when 500 mM Cl^- was added in, DTZ degradation was inhibited.

Eqs. (20) and (21) show the possible sinks for $SO_4^{\cdot-}$ and ·OH, although the reaction rate of $SO_4^{\cdot-}$ and ·OH are very high, there are also fast backward reactions. At low chloride concentration (1–100 mM), the scavenging effect of $SO_4^{\cdot-}$ by Cl^- was weak, mainly due to the backward reaction. However, high concentration of Cl^- (e.g., >300 mM) could favour the forward reaction of Eq. (20), leading to the consumption of sulfate radicals [56]. Thus, the inhibiting effect at 500 mM chloride concentration could be attributed to the scavenging of sulfate radicals by Cl^- to generate the less reactive species. The scavenging of $SO_4^{\cdot-}$ by Cl^- has already been studied by our laboratory, $Cl_2^{\cdot-}$ was found to be the main secondary radical [60].

$$Cl^- + SO_4^{\cdot-} \leftrightarrow Cl^{\cdot} + SO_4^{2-},\ k_f = 4.3 \times 10^8\ M^{-1}\ s^{-1},\ k_r = 2.5 \times 10^8\ M^{-1}\ s^{-1} \quad (20)$$

$$Cl^- + {}^{\cdot}OH \leftrightarrow ClOH^{\cdot-},\ k_f = 4.3 \times 10^9\ M^{-1}\ s^{-1},\ k_r = 6.1 \times 10^9\ M^{-1}\ s^{-1} \quad (21)$$

$$ClOH^{\cdot-} + H^+ \rightarrow Cl^{\cdot} + H_2O,\ k = 2.1 \times 10^{10}\ M^{-1}\ s^{-1} \quad (22)$$

$$Cl^{\cdot} + Cl^- \rightarrow Cl_2^{\cdot-},\ k = 8 \times 10^9\ M^{-1}\ s^{-1} \quad (23)$$

$$2Cl_2^{\cdot-} \rightarrow Cl_2 + 2Cl^-,\ k = 1.3 \times 10^9\ M^{-1}\ s^{-1} \quad (24)$$

3.4.3. Effect of bicarbonate

The impact of bicarbonate (concentration ranging from 0 to 40 mM) was also investigated in the present study at pH 8.2 (corresponding to 98% in the form HCO_3^-), and the results are displayed in Fig. 8. The presence of HCO_3^- induced promoting effect on simulated sunlight activated PS oxidation of DTZ, while the continuous increase of bicarbonate concentration did not lead to a rising trend of DTZ degradation efficiency. This result was unexpected and interesting, since bicarbonate generally played a negative role in AOPs due to the quenching ability of $SO_4^{\cdot-}$ and ·OH to form less reactive carbonate radicals ($HCO_3^{\cdot}$ and $CO_3^{\cdot-}$) [57]. Actually $CO_3^{\cdot-}$

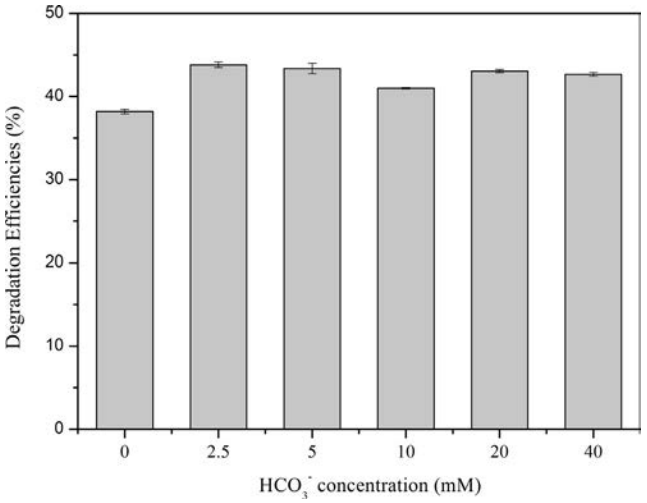

Fig. 8. Degradation efficiencies of DTZ by simulated sunlight activated PS in the presence of bicarbonate. ($[DTZ]_0$ = 30 mg L^{-1}, $[PS]_0$ = 12 mM, pH = 8.2, reaction time = 60 min, 10 mM Na_2HPO_4 and NaH_2PO_4 solutions were used to buffer the solutions).

could react with electron-rich compounds such as phenols and anilines at a fairly high rate [59].

$$HCO_3^- + SO_4^{\cdot-} \rightarrow H^+ + CO_3^{\cdot-} + SO_4^{2-},\ k = 2.8 \times 10^6\ M^{-1}\ s^{-1} \quad (25)$$

$$HCO_3^- + \cdot OH \rightarrow H_2O + CO_3^{\cdot-},\ k = 8.6 \times 10^6\ M^{-1}\ s^{-1} \quad (26)$$

In this study, the promoting effect of bicarbonate might be explained by the reaction between carbonate radical and DTZ. The second order rate constant of this reaction was detected as $5.4 \times 10^7\ M^{-1}\ s^{-1}$, which was less than that with $SO_4^{\cdot-}$ and ·OH. Since the concentration of bicarbonate was higher and $CO_3^{\cdot-}$ less reactive, a higher steady-state concentration of $CO_3^{\cdot-}$ was expected [44]. This counterbalanced the decrease level of $SO_4^{\cdot-}$ and ·OH due to carbonate scavenging and manifested a promoting effect on DTZ oxidation.

4. Conclusions

The present work shows that simulated sunlight could activate persulfate to produce $SO_4^{\cdot-}$ and induce the effective degradation of DTZ across a wide range of pH conditions (i.e. 4.5–8.5). Photo-activated PS was found to be more efficient as oxidant than H_2O_2. Sulfate radicals ($SO_4^{\cdot-}$) was found to be the dominant reactive species in the oxidation process, while, ·OH, was of less importance. The degradation was enhanced by the increasing of PS levels. The oxidation pathways included deiodination-hydroxylation, decarboxylation- hydroxylation and side chain cleavage. The initial step of DTZ degradation is the attack of $SO_4^{\cdot-}$, while the light-absorbing intermediates generated could take over. These observations highlight the formation of light-absorbing intermediate products and their involvement in the fate of ICMs in AOPs process.

In addition, DOM showed a detrimental effect on DTZ degradation while, a slight increase of DTZ decomposition was obtained in the presence of bicarbonate. Moreover, high concentration chloride inhibited the removal of DTZ. Our findings have potential environmental implications. For example, sulfate radical could react with naturally occurring constituents, such as bicarbonate and chloride and dissolved organic matter to form other types of reactive species. DOM is known as a sink of ·OH and $SO_4^{\cdot-}$, however, ·OH and $SO_4^{\cdot-}$ differ considerably in their reaction rates with DOM, ·OH reacts more quickly with DOM than $SO_4^{\cdot-}$. Thus, in natural waters (contained DOM), AOPs based on sulfate radicals seems more efficient than those based on hydroxyl radicals. However, this depends on the structure of target substrates. DOM could reduce the cation radicals of some contaminants to inhibit the oxidation, like anilines. Further studies should better consider the role of secondary reactive species (including light-absorbing intermediates) and the influence of naturally occurring constituents in natural waters.

Acknowledgements

Lei Zhou gratefully acknowledges the China Scholarship Council (CSC) for the financial support to study at IRCELYON (France).

Appendix A. Supplementary data

Supplementary data associated with this article can be found, in the online version, at http://dx.doi.org/10.1016/j.cej.2016.11.066.

References

[1] K. Kümmerer, Antibiotics in the aquatic environment–a review–part I, Chemosphere 75 (2009) 417–434.
[2] T. Heberer, Occurrence, fate, and removal of pharmaceutical residues in the aquatic environment: a review of recent research data, Toxicol. Lett. 131 (2002) 5–17.
[3] C.G. Daughton, T.A. Ternes, Pharmaceuticals and personal care products in the environment: agents of subtle change?, Environ Health Perspect. 107 (1999) 907.
[4] T.A. Ternes, A. Joss, H. Siegrist, Peer reviewed: scrutinizing pharmaceuticals and personal care products in wastewater treatment, Environ. Sci. Technol. 38 (2004) 392A–399A.
[5] T.A. Ternes, R. Hirsch, Occurrence and behavior of X-ray contrast media in sewage facilities and the aquatic environment, Environ. Sci. Technol. 34 (2000) 2741–2748.
[6] E. Mohle, C. Kempter, A. Kern, J. Metzger, Examination of the degradation of drugs in municipal sewage plants using liquid chromatography-electrospray mass spectrometry, Acta Hydroch. Hydrob. 27 (1999) 430–436.
[7] A.J. Watkinson, E.J. Murby, D.W. Kolpin, S.D. Costanzo, The occurrence of antibiotics in an urban watershed: From wastewater to drinking water, Sci. Total Environ. 407 (2009) 2711–2723.
[8] S. Ding, J. Niu, Y. Bao, L. Hu, Evidence of superoxide radical contribution to demineralization of sulfamethoxazole by visible-light-driven Bi2O3/Bi2O2CO3/Sr6Bi2O9 photocatalyst, J. Hazard. Mater. 262 (2013) 812–818.
[9] M. Klavarioti, D. Mantzavinos, D. Kassinos, Removal of residual pharmaceuticals from aqueous systems by advanced oxidation processes, Environ. Int. 35 (2009) 402–417.
[10] W. Xu, G. Zhang, S. Zou, X. Li, Y. Liu, Determination of selected antibiotics in the Victoria Harbour and the Pearl River, South China using high-performance liquid chromatography-electrospray ionization tandem mass spectrometry, Environ. Pollut. 145 (2007) 672–679.
[11] M.J. García-Galán, M.S. Díaz-Cruz, D. Barceló, Occurrence of sulfonamide residues along the Ebro river basin: removal in wastewater treatment plants and environmental impact assessment, Environ. Int. 37 (2011) 462–473.
[12] S. Pérez, D. Barceló, Fate and occurrence of X-ray contrast media in the environment, Anal. Bioanal. Chem. 387 (2007) 1235–1246.
[13] T. Reemtsma, M. Jekel, Organic Pollutants in the Water Cycle: Properties, Occurrence, Analysis and Environmental Relevance Of Polar Compounds, John Wiley and Sons Ltd, 2006.
[14] F. Sacher, F.T. Lange, H.J. Brauch, I. Blankenhorn, Pharmaceuticals in groundwaters: analytical methods and results of a monitoring program in Baden-Württemberg, Germany, J. Chromatogr. A 938 (2001) 199–210.
[15] C. Abegglen, A. Joss, C.S. McArdell, G. Fink, M.P. Schlüsener, T.A. Ternes, H. Siegrist, The fate of selected micropollutants in a single-house MBR, Water Res. 43 (2009) 2036–2046.
[16] W. Seitz, W.H. Weber, J.-Q. Jiang, B.J. Lloyd, M. Maier, D. Maier, W. Schulz, Monitoring of iodinated X-ray contrast media in surface water, Chemosphere 64 (2006) 1318–1324.
[17] A. Putschew, S. Wischnack, M. Jekel, Occurrence of triiodinated X-ray contrast agents in the aquatic environment, Sci. Total Environ. 255 (2000) 129–134.
[18] K. Kümmerer, T. Erbe, S. Gartiser, L. Brinker, AOX—Emissions from hospitals into municipal waste water, Chemosphere 36 (1998) 2437–2445.
[19] H.D. Humes, D.A. Hunt, M.D. White, Direct toxic effect of the radiocontrast agent diatrizoate on renal proximal tubule cells, Am. J. Physiol-Renal. 252 (1987) F246–F255.
[20] M.E. Gale, A.H. Robbins, R.J. Hamburger, W. Widrich, Renal toxicity of contrast agents: iopamidol, iothalamate, and diatrizoate, Am. J. Roentgenol. 142 (1984) 333–335.
[21] K.C. Huang, R.A. Couttenye, G.E. Hoag, Kinetics of heat-assisted persulfate oxidation of methyl tert-butyl ether, MTBE, Chemosphere 49 (2002) 413–420.
[22] M. Ahmad, A.L. Teel, R.J. Watts, Persulfate activation by subsurface minerals, J. Contam. Hydrol. 115 (2010) 34–45.
[23] L. Zhou, W. Zheng, Y. Ji, J. Zhang, C. Zeng, Y. Zhang, Q. Wang, X. Yang, Ferrous-activated persulfate oxidation of arsenic (III) and diuron in aquatic system, J. Hazard. Mater. 263 (2013) 422–430.
[24] O.S. Furman, A.L. Teel, R.J. Watts, Mechanism of base activation of persulfate, Environ. Sci. Technol. 44 (2010) 6423–6428.
[25] C.C. Lin, L.T. Lee, L.J. Hsu, Performance of UV/S2O82−process in degrading polyvinyl alcohol in aqueous solutions, in: J. Photochem. Photobiol. A 252 (2013) 1–7.
[26] Y. Wu, A. Bianco, M. Brigante, W. Dong, P. de Sainte-Claire, K. Hanna, G. Mailhot, Sulfate radical photogeneration using Fe-EDDS: influence of critical parameters and naturally occurring scavengers, Environ. Sci. Technol. 49 (2015) 14343–14349.
[27] J. Lu, J. Wu, Y. Ji, D. Kong, Transformation of bromide in thermo activated persulfate oxidation processes, Water Res. 78 (2015) 1–8.
[28] P. Neta, R.E. Huie, A.B. Ross, Rate constants for reactions of inorganic radicals in aqueous solution, J. Phys. Chem. Ref. Data 17 (1988) 1027–1284.
[29] R.E. Huie, C.L. Clifton, P. Neta, Electron transfer reaction rates and equilibria of the carbonate and sulfate radical anions, Radiat. Phys. Chem. 38 (1991) 477–481.
[30] H.V. Lutze, S. Bircher, I. Rapp, N. Kerlin, R. Bakkour, M. Geisler, C. von Sonntag, T.C. Schmidt, Degradation of chlorotriazine pesticides by sulfate radicals and the influence of organic matter, Environ. Sci. Technol. 49 (2015) 1673–1680.
[31] Y. Ji, C. Dong, D. Kong, J. Lu, New insights into atrazine degradation by cobalt catalyzed peroxymonosulfate oxidation: kinetics, reaction products and transformation mechanisms, J. Hazard. Mater. 285 (2015) 491–500.
[32] M.M. Huber, S. Canonica, G.-Y. Park, U. Von Gunten, Oxidation of pharmaceuticals during ozonation and advanced oxidation processes, Environ. Sci. Technol. 37 (2003) 1016–1024.

[33] F.J. Real, F.J. Benitez, J.L. Acero, J.J. Sagasti, F. Casas, Kinetics of the chemical oxidation of the pharmaceuticals primidone, ketoprofen, and diatrizoate in ultrapure and natural waters, Ind. Eng. Chem. Res. 48 (2009) 3380–3388.
[34] T.E. Doll, F.H. Frimmel, Kinetic study of photocatalytic degradation of carbamazepine, clofibric acid, iomeprol and iopromide assisted by different TiO 2 materials—determination of intermediates and reaction pathways, Water Res. 38 (2004) 955–964.
[35] W. Kalsch, Biodegradation of the iodinated X-ray contrast media diatrizoate and iopromide, Sci. Total Environ. 225 (1999) 143–153.
[36] A. Haiß, K. Kümmerer, Biodegradability of the X-ray contrast compound diatrizoic acid, identification of aerobic degradation products and effects against sewage sludge micro-organisms, Chemosphere 62 (2006) 294–302.
[37] I. Velo-Gala, J.J. López-Peñalver, M. Sánchez-Polo, J. Rivera-Utrilla, Comparative study of oxidative degradation of sodium diatrizoate in aqueous solution by H2O2/Fe2+, H2O2/Fe3+, Fe(VI) and UV, H2O2/UV, K2S2O8/UV, Chem. Eng. J. 241 (2014) 504–512.
[38] M.N. Sugihara, D. Moeller, T. Paul, T.J. Strathmann, TiO2-photocatalyzed transformation of the recalcitrant X-ray contrast agent diatrizoate, Appl. Catal. B-Environ. 129 (2013) 114–122.
[39] J. Jeong, J. Jung, W.J. Cooper, W. Song, Degradation mechanisms and kinetic studies for the treatment of X-ray contrast media compounds by advanced oxidation/reduction processes, Water Res. 44 (2010) 4391–4398.
[40] Y. Ji, Y. Fan, K. Liu, D. Kong, J. Lu, Thermo activated persulfate oxidation of antibiotic sulfamethoxazole and structurally related compounds, Water Res. 87 (2015) 1–9.
[41] C. Liang, Z.-S. Wang, C.J. Bruell, Influence of pH on persulfate oxidation of TCE at ambient temperatures, Chemosphere 66 (2007) 106–113.
[42] G.D. Fang, D.D. Dionysiou, D.M. Zhou, Y. Wang, X.D. Zhu, J.X. Fan, L. Cang, Y.J. Wang, Transformation of polychlorinated biphenyls by persulfate at ambient temperature, Chemosphere 90 (2013) 1573–1580.
[43] M. Quintiliani, P. Betto, J. Davies, M. Ebert, Radiation studies of iodinated benzoic acids, Radiat. Biolol. Chem. (1979).
[44] R. Zhang, P. Sun, T.H. Boyer, L. Zhao, C.H. Huang, Degradation of pharmaceuticals and metabolite in synthetic human urine by UV, UV/H2O2, and UV/PDS, Environ. Sci. Technol. 49 (2015) 3056–3066.
[45] H. Hori, A. Yamamoto, E. Hayakawa, S. Taniyasu, N. Yamashita, S. Kutsuna, H. Kiatagawa, R. Arakawa, Efficient decomposition of environmentally persistent perfluorocarboxylic acids by use of persulfate as a photochemical oxidant, Environ. Sci. Technol. 39 (2005) 2383–2388.
[46] D. Salari, A. Niaei, S. Aber, M.H. Rasoulifard, The photooxidative destruction of CI Basic Yellow 2 using UV/S2O82− process in a rectangular continuous photoreactor, J. Hazard. Mater. 166 (2009) 61–66.
[47] Y. Gao, N. Gao, Y. Deng, Y. Yang, Y. Ma, Ultraviolet (UV) light-activated persulfate oxidation of sulfamethazine in water, Chem. Eng. J. 195 (2012) 248–253.
[48] G.P. Anipsitakis, D.D. Dionysiou, Radical generation by the interaction of transition metals with common oxidants, Environ. Sci. Technol. 38 (2004) 3705–3712.
[49] M.G. Antoniou, A. Armah, D.D. Dionysiou, Degradation of microcystin-LR using sulfate radicals generated through photolysis, thermolysis and e− transfer mechanisms, Appl. Catal. B-Environ. 96 (2010) 290–298.
[50] Y.H. Guan, J. Ma, Y.M. Ren, Y.L. Liu, J.Y. Xiao, L. Lin, C. Zhang, Efficient degradation of atrazine by magnetic porous copper ferrite catalyzed peroxymonosulfate oxidation via the formation of hydroxyl and sulfate radicals, Water Res. 47 (2013) 5431–5438.
[51] J.J. Pignatello, E. Oliveros, A. MacKay, Advanced oxidation processes for organic contaminant destruction based on the Fenton reaction and related chemistry, Crit. Rev. Environ. Sci. Technol. 36 (2006) 1–84.
[52] M. Nie, Y. Yang, Z. Zhang, C. Yan, X. Wang, H. Li, W. Dong, Degradation of chloramphenicol by thermally activated persulfate in aqueous solution, Chem. Eng. J. 246 (2014) 373–382.
[53] J. Goldstone, M. Pullin, S. Bertilsson, B. Voelker, Reactions of hydroxyl radical with humic substances: bleaching, mineralization, and production of bioavailable carbon substrates, Environ. Sci. Technol. 36 (2002) 364–372.
[54] R.P. Schwarzenbach, P.M. Gschwend, D.M. Imboden, Environmental Organic Chemistry, John Wiley and Sons Ltd, 2005.
[55] E.M.L. Janssen, P.R. Erickson, K. McNeill, Dual roles of dissolved organic matter as sensitizer and quencher in the photooxidation of tryptophan, Environ. Sci. Technol. 48 (2014) 4916–4924.
[56] J. Wenk, S. Canonica, Phenolic antioxidants inhibit the triplet-induced transformation of anilines and sulfonamide antibiotics in aqueous solution, Environ. Sci. Technol. 46 (2012) 5455–5462.
[57] Y. Yang, J.J. Pignatello, J. Ma, W.A. Mitch, Comparison of halide impacts on the efficiency of contaminant degradation by sulfate and hydroxyl radical-based advanced oxidation processes (AOPs), Environ. Sci. Technol. 48 (2014) 2344–2351.
[58] C. Liang, Z.S. Wang, N. Mohanty, Influences of carbonate and chloride ions on persulfate oxidation of trichloroethylene at 20 °C, Sci. Total Environ. 370 (2006) 271–277.
[59] J. Huang, S.A. Mabury, A new method for measuring carbonate radical reactivity toward pesticides, Environ. Toxicol. Chem. 19 (2000) 1501–1507.
[60] C. George, J.-M. Chovelon, A laser flash photolysis study of the decay of SO4- and Cl2- radical anions in the presence of Cl- in aqueous solutions, Chemosphere 47 (2002) 385–393.
[61] A. Ghauch, A.M. Tuqan, N. Kibbi, S. Geryes, Methylene blue discoloration by heated persulfate in aqueous solution, Chem. Eng. J. 213 (2012) 259–271.
[62] Y. Guo, J. Zhou, X. Lou, R. Liu, D. Xiao, C. Fang, Z. Wang, J. Liu, Enhanced degradation of Tetrabromobisphenol A in water by a UV/base/persulfate system: kinetics and intermediates, Chem. Eng. J. 254 (2014) 538–544.